Hindawi Publishing Corporation
Mathematical Problems in Engineering
Volume 2012, Article ID 595823, 15 pages
doi:10.1155/2012/595823

Research Article

Signal Transceiver Transit Times and Propagation Delay Corrections for Ranging and Georeferencing Applications

P. Kaufmann,[1] P. L. Kaufmann,[2] S. V. D. Pamboukian,[3] and R. Vilhena de Moraes[4]

[1] *CRAAM, Escola de Engenharia, Universidade Presbiteriana Mackenzie, 01302-907 São Paulo, SP, Brazil*
[2] *Instituto de Matemática e Estatística, Universidade de São Paulo, 05508-090 São Paulo, SP, Brazil*
[3] *Laboratório de Geotecnologias e CRAAM, Escola de Engenharia, Universidade Presbiteriana Mackenzie, São Paulo, SP, Brazil*
[4] *Instituto de Ciência e Tecnologia, Universidade Federal do Estado de São Paulo, 12231-280 São José dos Campos, SP, Brazil*

Correspondence should be addressed to P. Kaufmann, pierrekau@gmail.com

Received 11 May 2012; Revised 20 July 2012; Accepted 10 August 2012

Academic Editor: Xi-Ming Sun

The accuracy of ranging measurements depends critically on the knowledge of time delays undergone by signals when retransmitted by a remote transponder and due to propagation effects. A new method determines these delays for every single pulsed signal transmission. It utilizes four ground-based reference stations, synchronized in time and installed at well-known geodesic coordinates and a repeater in space, carried by a satellite, balloon, aircraft, and so forth. Signal transmitted by one of the reference bases is retransmitted by the transponder, received back by the four bases, producing four ranging measurements which are processed to determine uniquely the time delays undergone in every retransmission process. A minimization function is derived comparing repeater's positions referred to at least two groups of three reference bases, providing the signal transit time at the repeater and propagation delays, providing the correct repeater position. The method is applicable to the transponder platform positioning and navigation, time synchronization of remote clocks, and location of targets. The algorithm has been demonstrated by simulations adopting a practical example with the transponder carried by an aircraft moving over bases on the ground.

1. Introduction

A very well-known principle to determine indirectly the distance of a remote object utilizes the echo of a retransmitted signal. When applied to electromagnetic signals the accuracy of

this method depends entirely on the knowledge of temporal effects due to four principal causes: (a) the signal speed propagation the medium causing path length variations; (b) propagation time at instruments, cables and connectors at the transmission; (c) propagation time at instruments, cables and connectors at the final reception; (d) time of signal transit at the remote transponder, which distance is to be determined.

The cause (a) is generally well described by models for propagation in various media (ionosphere, troposphere) as well as in space (see e.g., [1–6], and references therein). The path length variations, however, depends on the elevation angle the object (carrying a repeater) is seen from the bases, which needs to be determined.

Causes (b) and (c) are measured directly, with the high accuracy depending on the quality of the instruments that are utilized. The cause (d) however is undetermined since the remote object, carrying the transponder, is inaccessible for direct measurements. It undergoes changes in its internal signal propagation physical characteristics, which can change with time, or for each sequence of signals used to determine its distance. There are various long distance wireless transmission options using electromagnetic waves, such as the radio waves. The signals are sent to great distances using retransmission repeating links. At these links the signals are received, may or may not be stored or processed, be amplified, and then retransmitted at a frequency which may be the same, or different from the incoming frequency. As mentioned before, the signal transit time at the transponder is affected by several sources.

Other known time changes on fast moving transponders may be neglected for velocities $\ll$ the speed of light, because they produce effects much smaller in comparison to propagation and delays at the repeater. We refer to Doppler path change caused by frequency shifts in the direction of the repeater [7] and to relativistic effects relative to the reference system containing the sites to which the distances are to be determined, which become further accentuated when the satellites move over distinct gravity potentials relative to the geoid [8, 9].

On the other hand, passive transponders, such as the signal scattering reflection by meteor trails in the VHF frequency band [7], may undergo significant phase delays which need to be taken into account for distance measurements.

The precise knowledge of the time changes at each signal interaction at the transponder is an essential requirement for accurate ranging measurements, and applications in remote positioning, navigation, and time synchronization.

The new method to determine delays compares the positions of a repeater in space referred to at least two distinct sets of three of the four reference bases on the ground, with known geographic coordinates. A range of tentative possible delay values is set in advance. For a single time-coded transmitted signal calculations of the repeater's position are performed for different values assigned to the delays for each set of three reference bases on the ground. We show that the delays become determined as the repeater's positions converge to the same value in relation to at least two distinct sets of three out of four ground-based reference bases, for every single time-coded transmitted pulse.

2. Time Delays Derived from the Repeater Positioning Referred to Ground Bases

The original concept system to determine a repeater's position in space adopted three reference ground bases and a transponder of radio signals in space. It could be a passive natural radio reflection by meteor trails in the sky [10], or active signal repeaters carried

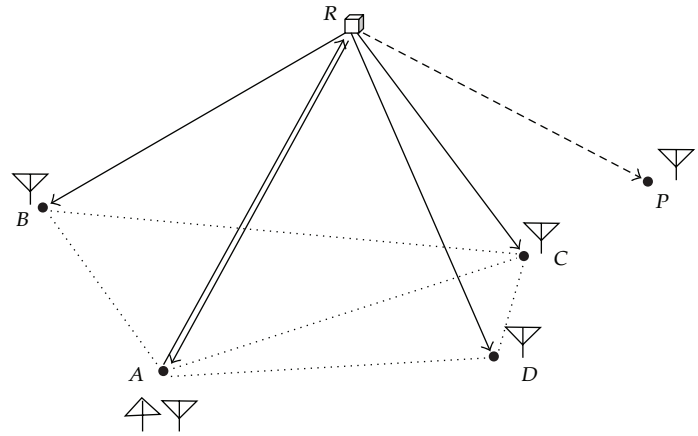

Figure 1: Simplified diagram showing the four reference bases on the ground A, B, C, D, the repeater R in the sky and the target P.

by space platforms [11]. A geometric calculation method has been proposed for particular situations and when all time delays are known in advance [12]. The complete resolving algorithm for those systems, irrespective from any particular geometry, has been developed [13]. This algorithm, however, is totally dependent on the previous knowledge of signal time changes at the repeater in space, and on time delays due to propagation in the medium (atmosphere, ionosphere), which in practice are not known.

A new method to determine the time variations at a repeater and signal propagation, for every signal interaction has been developed [14]. It overcomes the main difficulty limiting the practical use of the methods described before. The new system utilizes four reference bases on the ground (instead of three in the previous systems), A, B, C, and D, as illustrated in Figure 1, where R is the repeater in space, and P a target. All bases, and target P, are synchronized in time, to the best attainable accuracy.

At a given time, a coded signal is transmitted by reference base A, received and retransmitted by R, received back at A, at reference bases B, C, and D, as well as at target P. The ranging measurements obtained for that given instant can be written as

$$\begin{aligned}
AR\left(\delta_R, \Delta_{\mathrm{pd}AR}\right) &= \left(\Delta t_A - \delta_{At} - \delta_{Ar} - \delta_R\right)\left(\frac{c}{2}\right) - \Delta_{\mathrm{pd}AR},\\
BR\left(\delta_R, \Delta_{\mathrm{pd}AR}, \Delta_{\mathrm{pd}BR}\right) &= \left(\Delta t_B - \delta_{At} - \delta_{Br} - \delta_R\right)c - AR(\delta_R) - \Delta_{\mathrm{pd}BR} - \Delta_{\mathrm{pd}AR},\\
CR\left(\delta_R, \Delta_{\mathrm{pd}AR}, \Delta_{\mathrm{pd}CR}\right) &= \left(\Delta t_C - \delta_{At} - \delta_{Cr} - \delta_R\right)c - AR(\delta_R) - \Delta_{\mathrm{pd}CR} - \Delta_{\mathrm{pd}AR},\\
DR\left(\delta_R, \Delta_{\mathrm{pd}AR}, \Delta_{\mathrm{pd}DR}\right) &= \left(\Delta t_D - \delta_{At} - \delta_{Dr} - \delta_R\right)c - AR(\delta_R) - \Delta_{\mathrm{pd}DR} - \Delta_{\mathrm{pd}AR},\\
PR\left(\delta_R, \Delta_{\mathrm{pd}AR}, \Delta_{\mathrm{pd}PR}\right) &= \left(\Delta t_P - \delta_{At} - \delta_{Pr} - \delta_R\right)c - AR(\delta_R) - \Delta_{\mathrm{pd}PR} - \Delta_{\mathrm{pd}AR},
\end{aligned} \tag{2.1}$$

which are dependent on the time delay at the repeater δ_R and on the respective propagation paths delays $\Delta_{\mathrm{pd}AR}$, $\Delta_{\mathrm{pd}BR}$, $\Delta_{\mathrm{pd}CR}$, $\Delta_{\mathrm{pd}DR}$, and $\Delta_{\mathrm{pd}PR}$. AR, BR, CR, DR, and PR are the distances of bases A, B, C, D and of the target P to the repeater R, respectively, expressed as a function of time variations caused by the signal transit at the repeater δ_R, and corrected for

the respective propagation path delays. Δt_A, Δt_B, Δt_C, Δt_D, and Δt_P are the time differences effectively measured at bases A, B, C, and D, as well as at the target P, respectively, with respect to their clocks; δ_{At} is the time variation due to signal transit in circuits and cables when transmitted from base A, previously measured and known; δ_{Ar}, δ_{Br}, δ_{Cr}, δ_{Dr}, and δ_{Pr} are the time variations due to the signal transits on circuits and cables when received at bases A, B, C, D, and P, respectively, previously measured and known; c is the speed in free space of the electromagnetic waves that transport the coded time signal.

Since the repeater's position in the sky is not known in advance, the time variations δ_R at the repeater and the path delays are, in practice, determined simultaneously. As we determine δ_R, the approximate repeater's position is determined, and consequently the elevation angles seen from each one of the four bases are defined. These are needed to evaluate the propagation path delays for each distances AR, BR, CR, and DR. A propagation model in the medium must be selected to derive the delays and obtain the fully corrected repeater's position. Therefore the values for path delays $\Delta_{\mathrm{pd}AR}$, $\Delta_{\mathrm{pd}BR}$, $\Delta_{\mathrm{pd}CR}$, and $\Delta_{\mathrm{pd}DR}$ are added to the system of (2.1), which become a function of δ_R only. The value of $\Delta_{\mathrm{pd}PR}$ will be found similarly but afterwards, when the target position is to be determined.

The coordinates of the repeater platform R are defined in the reference system illustrated in Figure 2. The system of (2.1) expressed as a function of δ_R only can be resolved using the known nonrecursive algorithm [13], after which

$$
\begin{aligned}
x_R(\delta_R) &= \frac{\left\{[AR(\delta_R)]^2 - [BR(\delta_R)]^2 + AB^2\right\}}{[2AB]},\\
y_R(\delta_R) &= \left\{\frac{\left\{[r_1(\delta_R)]^2 - [r_2(\delta_R)]^2\right\}}{[2y_C]}\right\} + \frac{y_C}{2},\\
z_R(\delta_R) &= \left\{[r_1(\delta_R)]^2 - [y_R(\delta_R)]^2\right\}^{1/2},
\end{aligned}
\tag{2.2}
$$

where

$$
\begin{aligned}
[r_1(\delta_R)]^2 &= [AR(\delta_R)]^2 - [x_R(\delta_R)]^2,\\
[r_2(\delta_R)]^2 &= [CR(\delta_R)]^2 - [x_C - x_R(\delta_R)]^2.
\end{aligned}
\tag{2.3}
$$

On the other hand, adding the measurements obtained with bases A, B and D we get

$$
\begin{aligned}
x_R{}'(\delta_R) &= \frac{\left\{[AR(\delta_R)]^2 - [BR(\delta_R)]^2 + AB^2\right\}}{[2AB]} \quad \text{(equal to } x_R(\delta_R) \text{ in system (2.2))},\\
y_R{}'(\delta_R) &= \left\{\frac{\left\{[r_1{}'(\delta_R)]^2 - [r_2{}'(\delta_R)]^2\right\}}{[2y_D]}\right\} + \frac{y_D}{2},\\
z_R{}'(\delta_R) &= \left\{[r_1{}'(\delta_R)]^2 - [y_R{}'(\delta_R)]^2\right\}^{1/2},
\end{aligned}
\tag{2.4}
$$

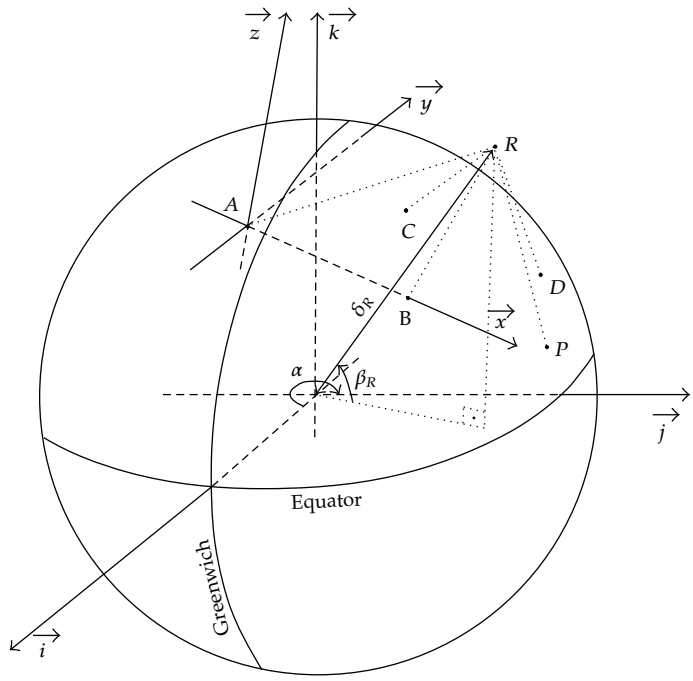

Figure 2: Spherical and Euclidean coordinate systems for the reference bases, A, B, C, and D, the repeater, R and the target P.

where

$$\begin{aligned} \left[r_1{}'(\delta_R)\right]^2 &= \left[AR(\delta_R)\right]^2 - \left[x_R{}'(\delta_R)\right]^2 \quad \left(\text{equal to } \left[r_1(\delta_R)\right]^2\right) \text{ in system (2.3)}, \\ \left[r_2{}'(\delta_R)\right]^2 &= \left[DR(\delta_R)\right]^2 - \left[\left(x_D - x_R{}'(\delta_R)\right]^2. \end{aligned} \tag{2.5}$$

The two pair of systems of (2.2) and (2.3), and (2.4) and (2.5) allow us to find the differences in position for the repeater as a function of δ_R [14]:

$$\begin{aligned} f(\delta_R) &= \left|\left[x_R(\delta_R), y_R(\delta_R), z_R(\delta_R)\right] - \left[x_R{}'(\delta_R), y_R{}'(\delta_R), z_R{}'(\delta_R)\right]\right|^2 \\ &= \left[x_R(\delta_R) - x_R{}'(\delta_R)\right]^2 + \left[y_R(\delta_R) - y_R{}'(\delta_R)\right]^2 + \left[z_R(\delta_R) - z_R{}'(\delta_R)\right]^2. \end{aligned} \tag{2.6}$$

The minimum value obtained for $f(\delta_R)$ with varying values of δ_R can be found by a number of well-known numerical calculation methods, such as by iterative procedures or by successive approximations, as it will be shown in the simulations later in this paper. The accuracy of δ_R determinations will be in the limit of the instrumental accuracies utilized for the coordinate's determination with the two system of (2.2) and (2.3), and (2.4) and (2.5). The same procedure may be repeated simultaneously, using measurements at bases A, C, and D, improving the accuracy by averaging the two independent estimates for δ_R.

The path delays for each distance AR, BR, CR, and DR, caused by propagation in the medium, $\Delta_{\text{pd}AR}$, $\Delta_{\text{pd}BR}$, $\Delta_{\text{pd}CR}$, and $\Delta_{\text{pd}DR}$, are derived at the same time redoing the

calculations using the respective elevation angles the repeater is seen from each one of the four bases, which were determined within a good approximation in the first set of calculations as a function of δ_R only.

The path delays are estimated by adopting an adequate propagation model, which differ for the frequency band used for the coded time signals transmissions. At higher SHF and EHF radio bands, for example, the corrections are primarily due to propagation in the lower atmosphere [2].The path delay corrections can be approximated using a plane parallel model for the atmosphere

$$\Delta_{\text{pd}} = \frac{c\tau_{\text{atm}}}{\sin H}, \tag{2.7}$$

where c is the speed of light, τ_{atm} the atmosphere zenith delay, and H the repeater's elevation angle with respect to the horizon as seen from the ground bases and by the target. At low frequency bands, at VHF and UHF and to a certain extent at L-band, the path delay corrections are mostly caused by propagation in the upper atmosphere, ionosphere, and plasmasphere [3].

3. Applications

3.1. Repeater's Navigation

The values of δ_R and of $\Delta_{\text{pd}AR}$, $\Delta_{\text{pd}BR}$, $\Delta_{\text{pd}CR}$, and $\Delta_{\text{pd}DR}$ found with this method are introduced in the system of (2.2) or (2.4) to obtain the repeater's actual coordinates, for each coded time interaction. The navigation of the platform is immediately derived from successive repeater's positions determinations.

3.2. Synchronism of a Remote Clock

Every transmitted coded time signal will be also received at other targets, as the example P given in Figure 1. Assuming that the position coordinates of P is known, once the coordinates of the repeater R are determined, the segment PR becomes known in advance. Therefore the discrepancy between the local clock at P and the time received from the clock at the transmitter A can be written as

$$\Delta t_P = \frac{AR}{c} + \frac{PR}{c} + \delta_{At} + \delta_R + \delta_{Pr} + \Delta_{\text{pd}AR} + \Delta_{\text{pd}PR}, \tag{3.1}$$

where the segments AR and PR are measured by ranging, δ_{At} and δ_{Pr} are experimentally determined and known, and δ_R, $\Delta_{\text{pd}AR}$, and $\Delta_{\text{pd}PR}$ are determined by the method described here. The clock time correction at P, needed for synchronization will be $\Delta t_p - \Delta_p$, where Δ_p is the theoretical correct time expected for the clock at position P.

One example to illustrate this application is shown in Figure 3. A repeater R is transported by an airplane, which is within the field of view of several actuators labeled L, M, N which geographic positions are known. These may be telecommunications retransmitters which essential requirement is to operate synchronized to prevent cross-talks and mutual message garbling interferences. The precision of clock corrections can be close to the accuracy attained in the synchronization of reference bases A, B, C, and D.

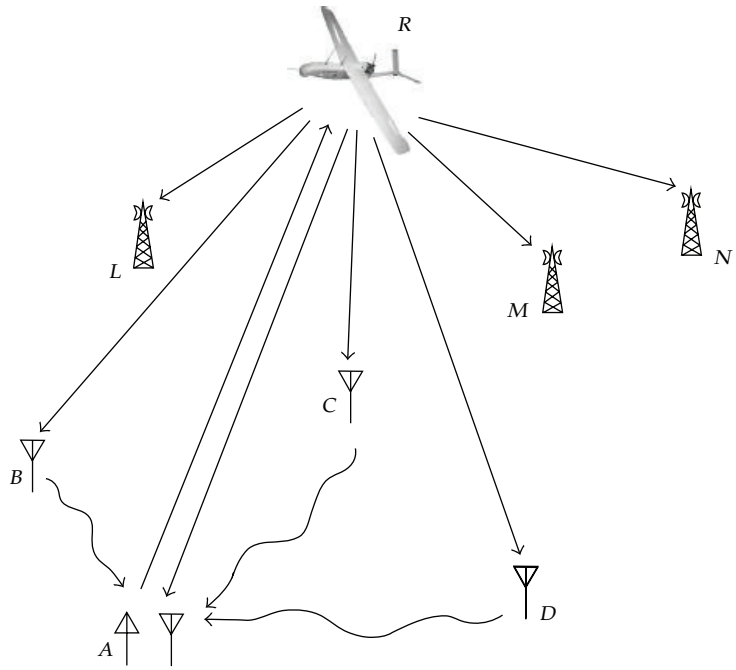

Figure 3: A time signal repeater R carried by an aircraft referred to reference bases A, B, C, and D, can synchronize remote actuators at known geographic positions L, M, and N.

3.3. Remote Target Location

We shall now assume that the remote target P (Figure 2) coordinates are not known and should be determined by this method. The distance from the repeater R, PR, can be determined by a single time interaction, provided that (a) the clock at P is sufficiently well synchronized with respect to the reference bases A, B, C, and D and (b) the temporal change of the coded time signal at the repeater δ_R and the propagation path delays are determined accordingly to the method demonstrated here. The coordinates of P can be determined univocally by obtaining four different measurements of its distance to the repeater R, located at four distinct positions and instants, provided that the respective repeaters' positions are not part of a straight line. The analytical procedures are the same given by Kaufmann et al. [13]. The calculations expressed by (2.1), (2.2), and (2.3) are repeated referring to one set of three reference bases, including A where the time code transmitter is located (i.e., A, B, C, or A, B, D, or A, C, D). We obtain the equations for four spheres which intersections give the coordinates of the target P.

4. Simulations

4.1. The Performance of the New System and Process

A new software has been developed to demonstrate the method performance and simulate practical measurements [15]. For the application we used the programming language of MATLAB software, version R2010a [16].

Table 1: Geographic precise locations and altitudes of reference bases and target used in simulations, illustrated in Figure 5.

City	Element	Latitude	Longitude	Altitude (m)
São Paulo	Base A	−23°32′51″	−46°37′33″	730
Itú	Base B	−23°15′51″	−47°17′57″	583
Campinas	Base C	−22°54′20″	−47°03′39″	855
Bragança Paulista	Base D	−22°57′07″	−46°32′31″	817
Atibaia	Target P	−23°07′01″	−46°33′01″	803

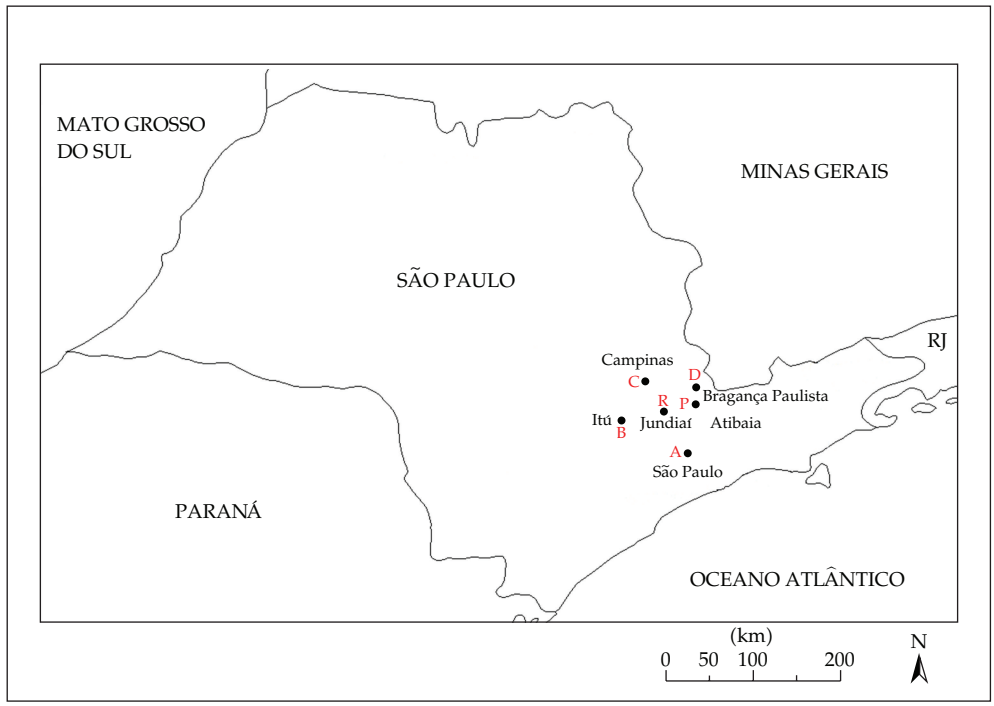

Figure 4: A Google map showing the preselected cities used in simulations, with reference bases A, B, C, and D and the target P. The repeater R is carried by an aircraft flying around the indicated city.

As a practical example, we conceived a regional framework, with a transponder carried by an aircraft. To represent the ground-based reference bases we have selected four cities in São Paulo state, Brazil: São Paulo, Itú, Campinas, and Bragança Paulista. The city of Atibaia, in the same state, has been selected to simulate the target P. The known locations for each city are shown in Table 1. The bases, target, and estimated location for the repeater are shown in map given in Figure 4. The aircraft with the transponder was flying at an altitude of about 6 km close to the city of Jundiaí, also shown in Figure 4. For simulation purpose, we arbitrarily assigned four positions for the aircraft/repeater, shown in Table 2.

To proceed with simulations the position coordinates shown in Tables 1 and 2 were converted into the ECEF (Earth-Centered, Earth-Fixed) coordinates system, using datum WGS84 [17–19] for the reference ellipsoid. The location of a point in this system can be done in coordinates (x, y, z). The origin of axes $(0, 0, 0)$ is the center of the Earth, the axis Z points to the North, axis X points to Greenwich meridian (where latitude = 0 degrees). The altitude

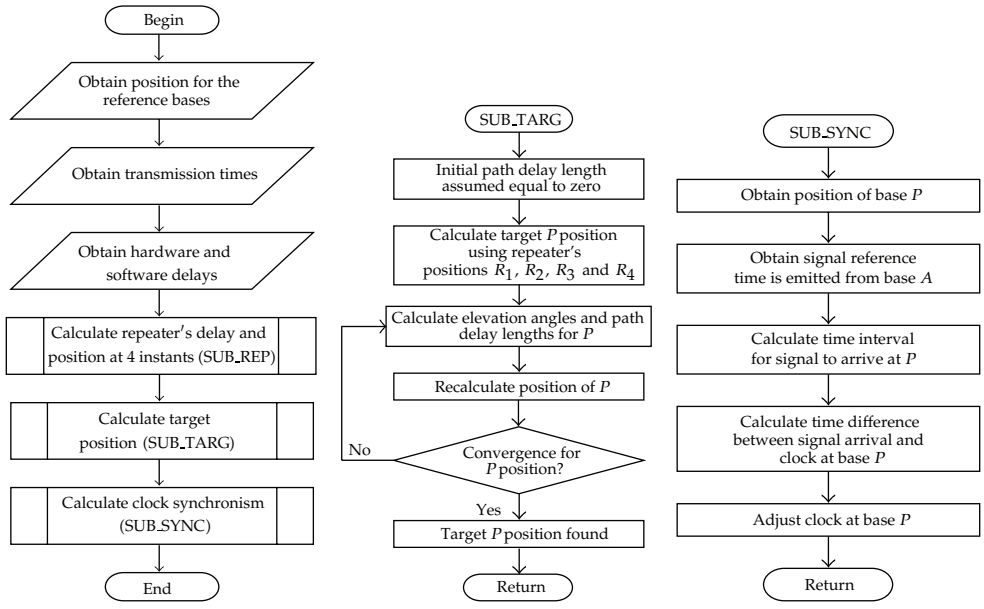

Figure 5: Flow diagrams showing the main routine (a), the target position calculation, (b) and clock synchronization (c).

is taken as the distance perpendicular and above the surface of the ellipsoid [17–19]. The flow diagrams utilized in the new software applications are shown in Figures 5 and 6.

For the simulations we have adopted a fixed value for the well-measured delays due to the signal passing through the electronics, cables, and connectors, both on transmission and on reception at each reference base and at the target. The same value was adopted for all prefixed delays, $\delta_{At}, \delta_{Ar}, \delta_{Ar}, \delta_{Br}, \delta_{Cr}, \delta_{Dr}, \delta_{Pr} = 0.0001\,\text{ms}$.

In order to compare with the simulated calculations, we have preestablished estimated values for the transmission times from the emitting base to the repeater, from the repeater to the reference bases and the target, for every successive repeater's positions. Adopting a hypothetical delay at the repeater equal to 200 ns (δ_R), $c = 299792458\,\text{m/s}$, the total times ($\Delta t_A$, Δt_B, Δt_C, Δt_D, and Δt_P) can be calculated the following system of equations (derived from (2.1)):

$$\begin{aligned}
\Delta t_A &= \frac{AR(\delta_R)}{c} + \frac{AR(\delta_R)}{c} + \delta_{At} + \delta_R + \delta_{Ar},\\
\Delta t_B &= \frac{AR(\delta_R)}{c} + \frac{BR(\delta_R)}{c} + \delta_{At} + \delta_R + \delta_{Ar},\\
\Delta t_C &= \frac{AR(\delta_R)}{c} + \frac{CR(\delta_R)}{c} + \delta_{At} + \delta_R + \delta_{Ar},\\
\Delta t_D &= \frac{AR(\delta_R)}{c} + \frac{DR(\delta_R)}{c} + \delta_{At} + \delta_R + \delta_{Ar},\\
\Delta t_P &= \frac{AR(\delta_R)}{c} + \frac{PR(\delta_R)}{c} + \delta_{At} + \delta_R + \delta_{Ar},
\end{aligned} \tag{4.1}$$

Table 2: The repeater's positions and altitudes carried by an aircraft, over the city of Jundiaí (see Figure 5).

City	Positions	Latitude	Longitude	Altitude (m)
Jundiaí	Position 1	−23°11′11″	−46°53′03″	5761
Jundiaí	Position 2	−23°11′11″	−46°59′03″	6000
Jundiaí	Position 3	−23°15′11″	−46°53′03″	6200
Jundiaí	Position 4	−23°15′11″	−46°59′03″	6800

Table 3: Simulated calculations for the repeater's positions, corrected for transit times and path delays added.

City	Positions	Latitude	Longitude	Altitude (m)
Jundiaí	Position 1	−23°11′10.99999999973079″	−46°53′03.00000000022578″	5761.0000008372590
Jundiaí	Position 2	−23°11′10.99999999990985″	−46°59′03.00000000035880″	6000.0000002672896
Jundiaí	Position 3	−23°15′11.00000000065677″	−46°53′03.00000000022578″	6200.0000010607764
Jundiaí	Position 4	−23°15′11.00000000052887″	−46°59′03.00000000110060″	6800.0000007525086

where the path delays were neglected in this step of the simulations. Adopting the information on the reference bases positions, delays at the bases, and transmission times, it was possible to simulate the whole process and determine the time delay at the repeater and its positions at four successive instants. Once the repeater's positions are determined it was possible to simulate the target position determination.

The first step was to calculate the repeater's position at the initial instant, using bases A, B, and C, according to (2.2) and (2.3), and adopting a given initial value for δ_R. In the next step the calculation was repeated using bases A, B, and D, according to (2.4) and (2.5), and, similarly, using bases A, C, and D. We will find three different positions for the repeater (R_1, R_2, and R_3) for each adopted value of δ_R. The error in the repeater's positioning has been calculated by the following equation:

$$\text{error} = \|R_1 - R_2\| + \|R_2 - R_3\| + \|R_3 - R_1\|. \tag{4.2}$$

This calculation (also known as objective function) has been repeated several times, for different adopted values of δ_R, using the MATLAB fmincon function, which provides the error minimization. The minimization process has been done starting with an initial value for δ_R and setting an upper and lower range for its variation. For this simulation we have adopted an initial value of 1 μs, with lower and upper limits of 0 and 100 μs, respectively. The correct time delay δ_R at the repeater is found at the end of the minimization process.

The whole process has been repeated for three more positions of the repeater, to allow the target position determination, using the known algorithm [13]. The results obtained were very close to the real preestablished values. The delay obtained at the repeater was of 199.999995 ns, very close to the preestablished value to obtain the transmission times (that was of 200 ns). The minimization process gave repeater's position error of about 0.001 mm.

Tables 3 and 4 show the simulated position calculations for the repeater and for the target, respectively. Comparing these results with the preestablished values set in Tables 1 and 2, we can see that the approximations are very good. The error in the target altitude, for example, is only 0.002 mm. Errors in latitude and longitude are less than 10^{-8} arcseconds. These initial calculations demonstrate the functionality of the method.

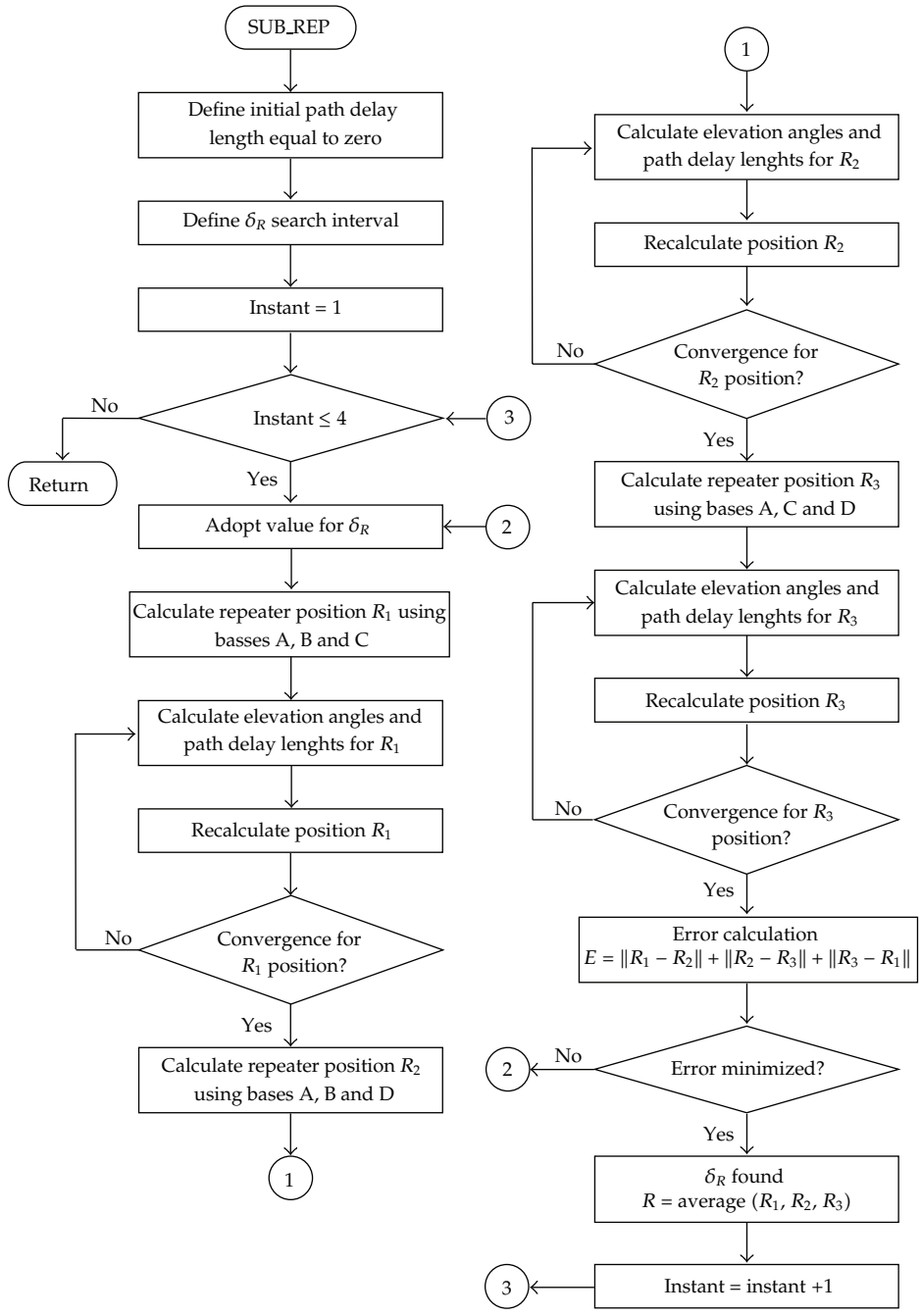

Figure 6: Flow diagram to calculate the transit time at the repeater, the path delays, and the repeater's position at four instants.

Table 4: Simulated calculations for the target position, corrected for transit times at the repeater and path delays added.

City	Latitude	Longitude	Altitude (m)
Atibaia	−23°07′00.99999999971089″	−46°33′00.99999999755028″	803.00000067241490

4.2. Estimate of Path Delays

The time delays due to the signal propagation in the medium were introduced in the following step. For the present simulations we shall assume radio frequencies in the range of several GHz (e.g., in the S band), for which the delays are dominated by propagation in the terrestrial troposphere. They can be approximately described by (2.7). We have assumed with Honma et al. [2] a typical sea level Δ_{pd} of about 2.3 m, for the dry component only. The calculations of delays at the repeater, of the repeater's position, and propagation path delays relative to each base were simulated by simultaneous iterations since there variable are interdependent.

With the initially adopted path delay equal to zero, the successive approximations in the minimization process allowed the determination of δ_R, for which the repeater's position was determined, as well as the elevation angles the repeater was observed from each reference base, and the respective path delay length calculated. The path delay lengths were then added to obtain a new position for the repeater. The process has been repeated until obtaining the convergence of values. Details on this process are shown in the flow diagram of Figure 6. Comparing the values found in this phase with the preestablished values we find that the approximations remain excellent, with discrepancies in the repeater's position and in the target position less than 10^{-3} mm (see Tables 3 and 4).

4.3. Clock Synchronism

The time of arrival of the transmitted time coded signal at a target with known coordinates permits the synchronization of the clock at that location. The time elapsed for the coded time signal to travel from the instant of transmission to the target at known position can be calculated using (3.1). The obtained time difference can be used to synchronize the target's clock to the clock at the transmitting base.

The results obtained from simulations are excellent. Assuming the clocks of the system perfectly synchronized, the ideal error at the receiving location is practically zero (i.e., less than 10^{-15} nanoseconds).

4.4. Estimate of Uncertainties

The practical source of uncertainties of the determinations is related to errors in clocks and/or in delays miscalculations. The two sources can be added together within a certain range of uncertainty.

To perform simulations on the clocks (and/or delays) uncertainties, we first set the determinations of δ_R and of path delays using the system and method described above. We have next generated random values for clock/delay uncertainties at the four reference bases and at the target, within a plausible time interval. The propagation of errors due to the clock synchronism uncertainties on the repeater's position, on the target location and on the clock synchronism, are exhibited in Figure 7 for ±5 ns, as an example. The plots correspond to 1000 randomly generated delay values, for four repeater's positions. For each delay it was determined the repeater's position, the target position and the clock synchronization accuracy. The most typical errors found for clock uncertainties of ±5 ns are of less than 2 meters in the repeater's position, of tens of meters for the target location, and of few ns on clock synchronization.

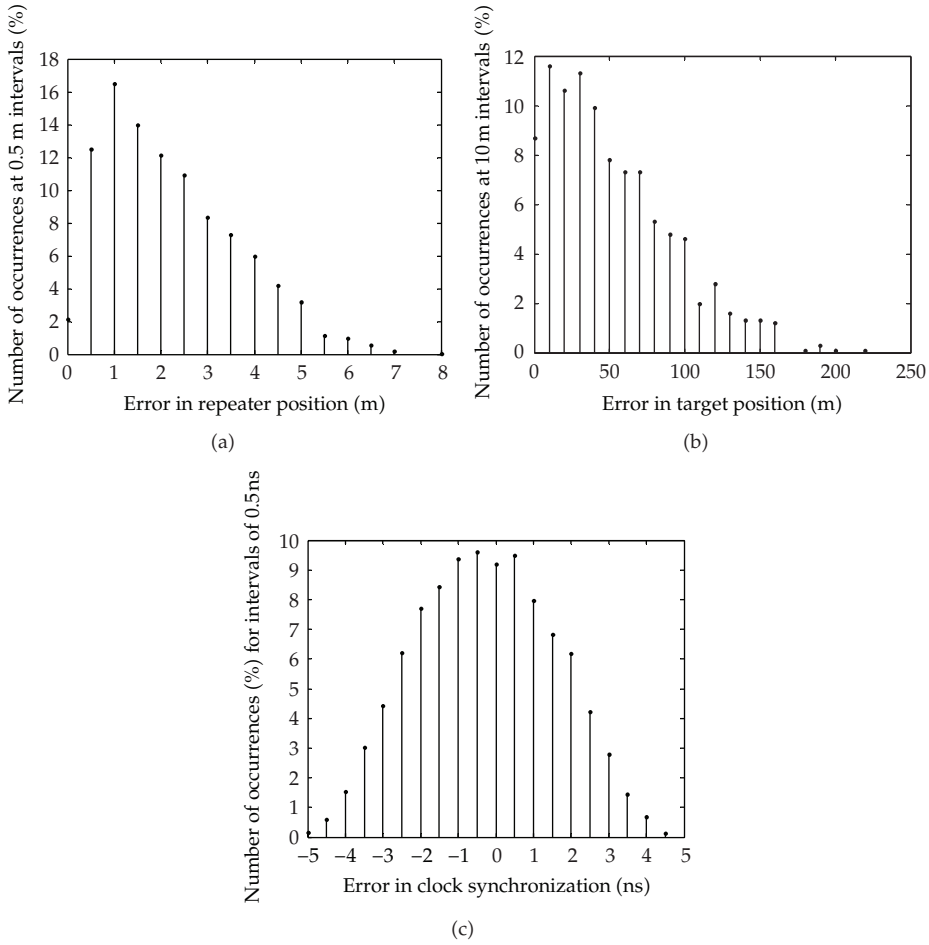

Figure 7: Example of errors caused by clock uncertainties, which may include the path delays errors, for a range of ±5 ns. In (a) the effect in the repeater position; (b) the error on the target location; (c) the error in clock synchronization.

4.5. Concluding Remarks

The present georeferencing system and method of calculations, using four reference bases at known locations on the ground and a remote transponder in space, permits the calculations of time delays of signals transiting by the repeater, and other caused by the signal propagation in the medium. The system and method allows the navigation of the repeater, remote target positioning and remote clock synchronization with very high accuracy. The simulations demonstrate the analytical performance of proposed algorithm on practical application with a transponder carried by an aircraft. The main sources of uncertainties are the clocks synchronism at the reference bases and the target.

The main scope of the system presented here is to make available an alternate method based on a concept distinct from other well-known georeferencing systems, such as the GPS and similar systems (which reference bases are at the satellites in the sky) and the Doppler based methods (based on velocity and range measured with respect of low orbit satellites

moving in relation to the targets). The new method may serve as a backup for the existing systems, at situations that require double checking of georeferencing parameters, but it can also function independently from the other.

Therefore the comparison between the simulated results obtained here with the new system and other systems must be taken as just illustrative, partial, and preliminary. The Doppler based systems, such Argos [20] require long time to make position determinations, because many measurements must be taken as the satellite moves to produce the location cones. The position uncertainties for a target, or inversely, for the satellite, are of the order or larger than hundred meters. The accuracy can be improved processing data for several orbital passes. These systems are not applicable for remote clock synchronization. The GPS system typical target positioning accuracies without processing are of the order of 15–30 meters [21]. The GPS clock synchronization best accuracies for civilian "unauthorized" are in the sub microsecond [22, 23]. It can be considerably improved with receivers employing dual frequency receivers [24]. The simulation of new method presented here, assumed arbitrarily a base and target clock synchronization ±5 ns. In this condition the method simulated performance is superior for remote clock synchronization. The target position determined with the new method requires four successive measurements (for a single repeater) exhibiting inaccuracies larger compared to GPS. However, it could be considerably improved, setting a better base and target clock synchronization. The comparison to GPS is not applicable for the repeater positioning, which is characteristic of the new method presented here.

A relevant application for this new system is the preliminary determination of satellite orbits. Assuming a repeater placed in an artificial satellite and a favorable geometry its position can be determined for every time mark interaction with the same errors or uncertainties found for repeaters at lower altitudes, shown here. A study on satellite orbital applications is currently being developed for future publication.

Acknowledgments

The authors acknowledge the remarks made by two referees, which were helpful to improve the paper presentation. This research was partially supported by Brazil agencies CNPq and CAPES.

References

[1] A. J. Anderson, "Path length variations due to changes in tropospheric refraction," in *Refractional Influences in Astrometry and Geodesy*, E. Tengstrom, G. Teleki, and I. Ohlsson, Eds., Symposium (International Astronomical Union), International Astronomical Union, no. 89, pp. 157–162, D. Reidel, Dordrecht, The Netherlands, 1979.

[2] M. Honma, Y. Tamura, and M. J. Reid, "Tropospheric delay calibrations for VERA," *Publications of the Astronomical Society of Japan*, vol. 60, no. 5, pp. 951–960, 2008.

[3] S. M. Hunt, S. Close, A. J. Coster, E. Stevens, L. M. Schuett, and A. Vardaro, "Equatorial atmospheric and ionospheric modeling at Kwajalein missile range," *Lincoln Laboratory Journal*, vol. 12, pp. 45–64, 2000.

[4] J. A. Klobuchar, "Design and characteristics of the GPS ionospheric time delay algorithm for single frequency users," in *Proceedings of the Position Location and Navigation Symposium (PLANS'86)*, pp. 280–286, IEEE, Las Vegas, Nev, USA, November 1986, Record (A87-41351 18-17).

[5] J. W. Marini, "Correction of satellite tracking data for an arbitrary tropospheric profile," *Radio Science*, vol. 7, pp. 223–231, 1974.

[6] T. S. Radovanovic, *Adjustment of satellite-based ranging observations and deformation monitoring [Ph.D. thesis]*, Department of Geomatics Engineering, University of Calgary, Calgary, Canada, 2002, Rept. Nr. 20166.

[7] M. I. Skolnick, *Introduction to Radar Systems*, McGraw-Hill, New York, NY, USA, 1962.

[8] N. Ashby, "Relativity and the global positioning system," *Physics Today*, vol. 55, no. 5, pp. 41–47, 2002.

[9] K. M. Larson, N. Ashby, C. Hackman, and W. Bertiger, "An assessment of relativistic effects for low Earth orbiters: The GRACE satellites," *Metrologia*, vol. 44, no. 6, pp. 484–490, 2007.

[10] P. Kaufmann, "Sistema e processo de posicionamento geográfico e navegação," Patent of Invention PI9101270-8, 1997.

[11] P. Kaufmann, "Sistema e processo de posicionamento geográfico e navegação," Patent Certificate of Addition C1910270-8, 2002.

[12] P. Kaufmann, "Geographic and space positioning system and process," Patent of Invention PI03003968-4, 2003, international PCT application filed on 4 October 2004, granted in USA, (US752877B2, 2009), Russia (RU2635934C2, 2009), Australia (AU2004277511, 2010), Canada (2010) and China (2011).

[13] P. L. Kaufmann, R. Vilhena de Moraes, H. K. Kuga, L. A. Beraldo, C. N. Motta Marins, and P. Kaufmann, "Non recursive algorithm for remote geolocation using ranging measurements," *Mathematical Problems in Engineering*, vol. 2006, Article ID 79389, 9 pages, 2006.

[14] P. Kaufmann P and P. Levit Kaufmann, "Process and system to determine temporal changes in retransmission and propagation of signals used to measure distances, synchronize actuators and georeference applications," Patent of Invention PI03003968-4, 2012, International PCT Application.

[15] S. V. D. Pamboukian, "Novo processo de georeferenciamento: determinação de posição de transponder romoto e aplicações no posicionamento de alvos e disseminação de tempos," Software registered in Brazil, protocol 020120032225, 2012.

[16] Mathworks, MATLAB—The Language of Technical Computing, 2012, http://www.mathworks.com/products/matlab/.

[17] P. H. Dana, *Geodetic Datum Overview*, 1995, http://www.colorado.edu/geography/gcraft/notes/datum/datum.html.

[18] European Organization for the Safety of Air Navigation and Institute of Geodesy and Navigation, *WGS 84 Implementation Manual—Version 2.4*, European Organization for the Safety of Air Navigation, Institute of Geodesy and Navigation, Brussels, Belgium, 1998.

[19] National Imagery and Mapping Agency, *Department of Defense World Geodetic System 1984: Its Definition and Relationships With Local Geodetic Systems*, National Imageryand Mapping Agency, Bethesda, Md, USA, 3rd edition, 1997, NIMA TR8350, http://earth-info.nga.mil/GandG/publications/tr8350.2/wgs84fin.pdf.

[20] C. S. Tobler de Sousa and H. K. Kuga, "Comparing INPE and ARGOS geo-location algorithms accuracies with ARGOS system real data," in *Advances in Space Dynamics 4: Celestial Mechanics and Astronautics*, H. K. Kuga, Ed., pp. 283–289, Instituto Nacional de Pesquisas Espaciais—INPE, São José dos Campos, Brazil, 2004.

[21] J. B. Zumberge and W. I. Bertinger, "Ephemeris and clock navigation message accuracy," in *Global Positioning System: Theory and Applications*, B. W. Parkinson and J. J. Spilker Jr., Eds., vol. 163, pp. 585–600, American Institute of Aeronautics and Astronautics, Cambridge, Mass, USA, 1996.

[22] T. A. Clark, R. M. Hambly, and R. Abtahi, "Low cost, high accuracy GPS timing," in *Proceedings of the ION Navigation's GPS Conference*, September 2000, http://www.gpstime.com/pub/ION-GPS2000/ion-time.

[23] J. C. Eidson, M. Fisher, and J. White, "IEEE standard for a precision clock synchronization protocol for networked measurement and control systems," in *Proceedings of the 34th Annual Precise Time and Time Interval (PTTI) Systems and Applications Meeting*, Reston, Va, USA, December 2002.

[24] M. A. Lombardi, L. M. Nelson, A. N. Novick, and V. S. Zhang, "Time and frequency measurements using global positioning system," *Cal Lab: The International Journal of Metrology*, pp. 26–33, 2001.